Title
Differentiating zones at periodontal ligament–bone and periodontal ligament–cementum entheses

Journal
Journal of Periodontal Research, 50(6)

ISSN
0022-3484

Authors
Lee, J-H
Pryce, BA
Schweitzer, R
et al.

Publication Date
2015-12-01

DOI
10.1111/jre.12281

Peer reviewed

HHS Public Access

Author manuscript

J Periodontal Res. Author manuscript; available in PMC 2016 December 01.

Published in final edited form as:

J Periodontal Res. 2015 December ; 50(6): 870–880. doi:10.1111/jre.12281.

Differentiating Zones at Periodontal Ligament-Bone and Periodontal Ligament-Cementum Entheses

Ji-Hyun Lee, DDS., Ph.D[1], **Brian A. Pryce**[2], **Ronen Schweitzer, Ph.D**[2], **Mark I. Ryder, DMD**[3], and **Sunita P. Ho, Ph.D**[1,*]

[1]Division of Biomaterials and Bioengineering, Department of Preventive and Restorative Dental Sciences, University of California, San Francisco, San Francisco, CA, USA

[2]Portland Shriner's Research Center, Oregon Health & Science University, Portland, OR, USA

[3]Division of Periodontology, Department of Orofacial Sciences, University of California, San Francisco, San Francisco, CA, USA

Abstract

Background and Objective—The structural and functional integrity of bone-periodontal ligament (PDL)-cementum complex stems from the load-bearing attachment sites (entheses) between soft (PDL) and hard (bone, cementum) tissues. These attachment sites are responsible for maintenance of a bone-PDL-cementum complex biomechanical function. The objective was to investigate changes in spatiotemporal expression of key biomolecules in developing and functionally active entheses.

Material and Methods—Multilabeling technique was performed on hemimandibles of 3 week and 3 month-old scleraxis (scx)-GFP transgenic mice for CD146, CD31, NG2, osterix (OSX), and bone sialoprotein (BSP). Regions of dominant stretch within the PDL were evaluated by identifying directionality of collagen fibrils, PDL fibroblasts, and PDL cell cytoskeleton.

Results—CD146+ cells adjacent to CD31+ vasculature were identified at PDL-bone enthesis. NG2+ cells were located at coronal bone-PDL and apical cementum-PDL entheses in the 3 weeks-old group, but at 3 months, NG2 was positive at the entheses of the apical region and alveolar crest. NG2 and OSX were colocalized at the osteoid and cementoid regions of the PDL-bone and PDL-cementum entheses. BSP was prominent at the apical region of 3 week old mice. The directionality of collagen fibers, fibroblasts, and their cytoskeleton overlapped, except in the apical region of 3 weeks.

Conclusion—Colocalization of biomolecules at zones of the periodontal ligament adjacent to attachment sites may be essential for the formation of precementum and osteoid interfaces at a load-bearing bone-PDL-tooth fibrous joint. Biophysical cues resulting from development and function can regulate recruitment and differentiation of stem cells potentially from vascular origin toward osteo- and cemento-blastic lineages at the PDL-bone and PDL-cementum entheses. Investigating the coupled effect of biophysical and biochemical stimuli leading to cell

Correspondence: Sunita P. Ho, Ph.D. Division of Biomaterials and Bioengineering, Department of Preventive and Restorative Dental Science, 707 Parnassus Avenue, D2252, University of California at San Francisco, San Francisco, CA 94143-0758, USA, Tel: +1 415 514 2818, Fax: +1 415 476 0858, sunita.ho@ucsf.edu.

differentiation at the functional attachment sites is critical for developing regeneration strategies to enable functional reconstruction of the periodontal complex.

Keywords

tissue entheses; periodontal ligament; tooth-bone biomechanics

Introduction

Biological interfaces are transition zones and contain sites that attach disparate or similar tissues (1). Attachment sites contain multiple cell types with biophysical and biochemical interplay between cells, organic and inorganic macromolecules (2, 3). Functional attachment sites are also termed as entheses where soft and hard tissues attach to regulate passive and/or active mechanical strains. Adjacent to the enthesis sites, there exists 10-15 μm wide zones rich in biochemical and biophysical gradients for multiple cell to cell and cell to globular and fibrillar protein interactions (4, 5). Biomechanically, these regions are of higher viscosity and exist in developing or functionally active load bearing organs. This enriched viscous environment is due to the presence of organic-rich and dynamic zones and can aid in regulating passive and active stretches within tissue and at their entheses through the lifespan of an organism

Analogous to the load bearing musculoskeletal systems in the body, the bone-periodontal ligament (PDL)-cementum complex functions through orchestrated events within and across multiple tissue types. The PDL, soft tissue, provides a natural ‘docking’ of hard cementum-lined dental roots within bony alveolar sockets. The PDL-bone and PDL-cementum attachment sites contain biomechanical gradients to facilitate load transfer from tooth to bone and to resist mechanical load. Although the concept of fibrocartilaginous attachment sites has been investigated in the musculoskeletal system (1), few studies have been performed on the enthesial sites of the bone-PDL-tooth fibrous joint. Despite common characteristics between the PDL-entheses and musculoskeletal entheses including biomolecules and interfacial mechanics, not all knowledge gained from studies on musculoskeletal system is directly applicable to the fibrous joint between tooth and alveolar bone due to the fundamental difference in mineralization of oral and craniofacial complex. Thus, the novel aspect of this study is, to investigate spatiotemporal changes in levels of key biomolecules at the enthesis zones in developing and functioning bone-PDL-cementum complexes.

Spatiotemporal mapping was necessary to characterize the importance of the enthesial zone, which is hypothesized to balance mineral forming and resorbing events to conserve joint function. The proof-of-concept for the aforementioned hypothesis is further strengthened by the mineral forming and resorption events as a result of the evolutionarily programmed innate mesial tooth drift in humans (6). These mechanisms of tooth drift exist throughout the age of other mammals and are reversed in direction in rats and mice (7), the two commonly used *in vivo* model systems. The consistent observation of the transient events at the entheses implies that the events can regulate properties of interfaces and prompt questions, such as; 1) are the population of cells and matrix molecules at the entheses different for

tissue-specific cells? 2) If so, what is their origination? The present study is designed to answer the first question that will be discussed from a biomechanics perspective by contrasting biophysical and biochemical results obtained from 3 weeks-old mice having a developing complex containing bone-PDL and cementum-PDL entheses with 3 month-old mice having a functionally active bone-PDL-tooth complex.

Biophysical cues play a critical role in the development of organs that contain ligaments and bones not only in musculoskeletal system but also the dentoalveolar complex (8-10). Extraneous loading may not be necessary to initiate enthesis development, but is required for the subsequent growth and maturation of the enthesis (11). In the same context, subsequent to the removal of all teeth in adults, the alveolar bone undergoes atrophy(12, 13). Given these findings, it is conceivable that the development of function-mediated stretches at the enthesis sites could be responsible for development and homeostasis of organ structure. In addition, the presence of various cell types and molecules at the attachment sites during development and function could also aid in providing shape memory, a much needed functional characteristic to conserve overall joint biomechanics. The objective of this study was to identify biochemical characteristics of the enthesial zones preceding ligament-bone and ligament-cementum attachment sites in a developing and a functionally active bone-PDL-tooth fibrous joint.

Hence, multilabelling technique to colocalize molecules was performed on the 3 week old periodontal complex of developing molars compared to functionally adapted complexes of 3 month old mice. These labeling approaches focused on a few molecules that are deemed necessary to consequently bring organic and inorganic constituents that form a functional enthesis for tooth development and movement in the bony socket. These molecules include, NG2 and CD146 which identify the locality of precursors relative to the blood vessels, osterix (osx) as a cell differentiation marker to detect blastic lineage, and bone sialoprotein (BSP), as a putative mechanosensor. In addition, it is postulated that the ligament-specific marker, scleraxis (scx) can be used to identify tension dominant regions and correlate them to expression of molecules specific to genesis of inorganic fronts. Detection of these molecules at the entheses and proposed enthesial zones was performed using transgenic scx-reporter mice. Moreover, overall change in morphology, cell population and the organic matrix composition of the complex, especially at the enthesis is described in the context of its ontogeny.

Material and Methods

Mice

The generation of ScxGFP transgenic reporter mice have been previously described (14). Mouse mandibles were harvested at 3 weeks and 3 months postnatally, and fixed in 1% paraformaldehyde, demineralized in 0.5M ethylene diaminetetraacetic acid (EDTA, pH 8.0) for 1 to 2 weeks at 4°C. Then, the mandibles were embedded and snap frozen in ethanol-dry ice as described previously (15).

Histochemistry and Immunofluorescence

The mandibles were serially sectioned in sagittal plane at 10 μm with a cryostat. Only mesial bone-PDL-cementum complex of the 2nd mandibular molar was investigated. Heat-based antigen retrieval was employed only for NG2, Osx and BSP staining before primary antibody incubation. Primary antibodies included rabbit anti-mouse CD146 (1:250, AB75769, Abcam, Cambridge, MA, USA), rabbit anti-mouse NG2 (1:100, AB5320, Chemicon, Temulca, CA, USA), rat anti-mouse CD31 (1:20, DIA-310, Dianova, Hamburg, Germany), rabbit anti-mouse Osterix (1:200, AB22252, Abcam, Cambridge, MA, USA), and BSP (1:100, sc-292394, Santa Cruz Biotechnology, Santa Cruz, CA, USA). Slides were then incubated in Alexa Fluor 594 donkey anti-rabbit or Alexa Fluor 647 goat anti-rat secondary antibody (Molecular Probes, Eugene, OR, USA) at a 1:200 dilution and counterstained with Hoechst 33342. For staining of the actin cytoskeleton, rhodamine-conjugated Phalloidin (5ul/ml, Cytoskeleton Inc., Denver, CO, USA) was used. Procedures for picrosirius red staining (PSR) were done as previously described (16).

Histomorphometry and statistical analysis

In order to verify the vicinity of CD31 and CD146 expression to either bone-PDL or cementum-PDL interfaces, fluorescence intensity was measured and calculated per area within 25um, 50um, and 100um from B to PDL interface within the PDL. CD146/CD31 intensity measurements were statistically analyzed. The one-way repeated measures Analysis of Variance (ANOVA) was employed for CD146/CD31 data to disclose the difference depending on the distance from the interface, using SPSS 16.0. For adjustment for multiple comparisons, the Bonferroni post hoc test was used to reveal which specific means differed. Significance was determined at p value of 0.05.

Results

Distribution and colocalization of capillaries and CD146+ cells

CD146, was colocalized with a thin endothelial lining identified by CD31. Expression of CD146 was detected adjacent to capillaries through subgingival connective tissue, PDL-space, dental pulp, endosteal space, and bone marrow (Fig. 1A and 1B). In both 3 week and 3 month-old mice, the distribution of CD31 and CD146 was observed in the vicinity of bone-PDL interface. The fluorescent intensity of CD31 and CD146 at 25μm, 50μm was significantly higher than and 100μm from bone-PDL interface ($p<0.5$, Fig 2). Because PDL width in mice at each age was not beyond 100 μm, the intensity was measure only within 100 μm.

NG2+ cells, not in spatial concordance with CD146+ cells

NG2+ cells were observed in proximity of endothelial cell in vasculature, parallel to CD146. However, the distribution of NG2+ cells was different from CD146+ cells; they were also observed along bone-PDL and cementum-PDL interface (Fig 3 and 4). The pattern of distribution between the two interfaces was different. At bone-PDL interface, more NG2+ cells were located coronally but not apically at 3 weeks (Fig. 4B and 4C arrowheads, S1), but 3 months-old group showed increased NG2 expression in apical region as well as on the

alveolar crest (Fig. 4F and 4G, S1). On the other hand, at cementum-PDL interface of 3 weeks-old group, NG2+ cells were concentrated in actively developing secondary cementum of the apical portion of the root (Fig. 4C, S1). This pattern was also observed in 3 months-old group but not as obvious as in 3 weeks-old group (Fig. 4E through 4H, S1).

Osterix, the prime suspect to confirm the phenotype of NG2+ cells observed at bone-PDL and cementum-PDL attachment sites

NG2+ cells were observed in perivascular regions, but another set of NG2+ set was found along interface, which doesn't meet the definition of pericyte, a mural cell wrapping endothelial cells composing wall of vasculature. Judging from the fact that their locality is exclusively at PDL attachment site to alveolar bone and cellular cementum, they are presumed to be osteoblast- and cementoblast-lineage. Therefore, temporal and spatial expression pattern of osterix (Osx), which is a transcription factor essential for osteogenesis (17, 18) and potentially cementogenesis (19, 20), was mapped on the serial sections to NG2 stained ones.

Immunofluorescent staining showed that at 3 weeks, Osx was expressed in the cell lining alveolar bone and cellular cementum (Fig. 4I through 4L). As seen in NG2 staining, Osx was also negative at apical bone-PDL interface (Fig. 4K arrowheads). At 3 months, Osx expression at bone-PDL interface was similar to the spatial location of NG2+ cells. However, no Osx+ cells at cementum-PDL interface were observed (Fig. 4O). Immunoreactivity of Osx was also observed in odontoblasts lining dental pulp chamber, bone marrow stromal cells and PDL cells within PDL space, although the fluorescence signal was weaker at 3 months than at 3 weeks.

Bone Sialoprotein, prominent in mineralized tissues, especially at the matrix-matrix interfaces

Anti-BSP antibody stained all the mineralized structures within the complex. To be specific, immunoreactivity for BSP was observed in acellular and cellular cementum as well as alveolar bone, while only weak staining was observed in predentin layer. Coronal region showed patched and dispersed BSP expression (Fig 5A, 5D) as if it was a sum of numerous mineralization foci, whereas BSP was prominent in the cement lines in apical region (Fig, 5B, 5E). At 3 weeks, rich BSP expression along the cemental lines was noticed on the apical bone-PDL interface (Fig. 5B arrowheads) but the apical bone-PDL interface at 3 months lacked BSP immunolabeling (Fig. 5E arrowheads).

Directionality of strain governing PDL, displayed on collagen fibers, fibroblasts and cytoskeleton within PDL space

PSR staining and polarized light microscopy revealed collagen fiber orientation highlighted by birefringence. ScxGFP was utilized to identify the location and shape of PDL fibroblasts (21). To further identify the orientation of cytoskeleton and correlate it with the angular distribution of PDL fibroblasts and collagen fibers, phalloidin was employed to stain cytoplasmic actin filaments.

At 3 weeks, the angular distribution of collagen fibers, fibroblasts, and PDL cell cytoskeleton coincides within PDL complex in coronal region (Fig. 6A, 6i) but not in apical region (Fig. 6A, 6ii); collagen fibers run perpendicularly to cellular cementum with less birefringence, while the orientation of actin filaments and fibroblasts is oblique toward root apex. At 3 months, collagen fibers, PDL fibroblasts, and PDL cell cytoskeleton concurs in the directionality both coronally and apically (Fig 6B, 6iii and 6iv), although the distribution of actin filaments was less aligned than collagen fibers and PDL fibroblast. In comparison to 3 weeks, collagen fibers and PDL fibroblasts manifested in stronger and more uniformed alignment at 3 months.

Discussion

Accounting for functional significance of the bone-PDL-tooth complex, attempts have long been made to exploit the principle underlying healing and regeneration of injured and/or diseased complexes. Evolved from introduction of filler materials into alveolar bony defect aiming at the newer bone formation, more attention is given to the technique to guide and instruct the reserved progenitors of the PDL to utilize self-contained regenerative capacity. However, adaptive change of the complex resulting from mechanical and pathologic insults is pronounced at the PDL attachment site to alveolar bone and cementum and manifested as constant renewal of organic and inorganic constituent to conserve PDL space and maintain the functional and structural integrity. In this study, therefore, we propose that the bone-PDL and cementum-PDL entheses contain biophysical and biochemical “blue prints” for regeneration and it has much to do with biophysical amplification at the attachment sites.

The PDL is distinct from skeletal ligaments because it is vascularized and innervated (22). Density of capillary network is also a unique feature at the bone remodeling site (23) and the cells intercalated with vasculature named pericytes have been proven to be enriched with tissue-resident mesenchymal stem cells (MSCs) (24, 25). Therefore, it is hypothesized that the perivascular niche within PDL space, preferentially along the attachment sites, fuel the development of enthesial zones identified as osteoid and cementoid within bone-PDL-cementum complex. In spite of the heterogeneity within MSC population and lack of consensus on the MSC phenotype, pericyte markers were employed to identify the MSCs niche. Recent studies utilizing in vivo lineage tracing technology (26-28) and cell isolation with in vitro culture (29, 30) indicated that perivascular cell populations positive of CD146, NG2 and αSMA differentiate into mature mesenchymal tissues within periodontal complex. The pericyte markers included in this study are CD146, one of the adult MSC marker, expressed on pericytes (31-33) and NG2, a chondroitin sulfate proteoglycan that is commonly used as a marker for pericytes (34) and has been proposed to represent a population of MSCs in the dental mesenchyme (27, 35). CD31, also known as platelet endothelial cell adhesion molecule-1 (PECAM-1), was chosen to localize vasculature within the complex.

The CD146/CD31 colocalization showed that the prevalence of CD146+ cells in the PDL space follows the same pattern as the distribution of vasculature along the bone-PDL attachment site (Fig. 1 and 2). This finding is in line with previous works on vessel distribution in relation to bone surface (23, 36). The distribution of vasculature indicated by

CD31+ cells was partial to bone-PDL interface, rather than cementum-PDL interface, although both are mechanically active entheses. The difference in blood vessel density and prevalence of putative stem cells as identified as CD146+ implies a distinct source to fuel development and maintenance of each tissue. Bone undergoes continuous remodeling through life to maintain its volume and shape through a tight regulation of osteoblasts, osteocytes, and osteoclasts (37). Additionally, vascular invagination is essential for regeneration and repair that predominantly involves migration of osteoclastic and osteoblastic progenitors (38). Furthermore, osteoclasts are of hematopoietic lineage and its differentiation involves multiple steps associated with cytokines such as RANKL and OPG (39). In contrast, cementum does not undergo remodeling under healthy conditions, albeit signals from the attached PDL could likely influence cementoblast function (40). Based on these observations, it can be postulated that bone requires a tight-knit assistance from hematopoietic environments although bone *per se* originated from mesenchymal lineage. However, it appears that the local environment of cementum matrix plays a pivotal role in maintaining cementum homeostasis and in turn the needed functional space for conserved tooth movement in the bony socket (41).

NG2 was observed at two different locations: immediately adjacent to endothelial cells, and at bone-PDL and cementum-PDL entheses (Fig. 3 and 4). NG2+ cells populated along the bone-PDL and cementum-PDL attachment sites cannot be considered as perivascular mesenchymal stem cells due to the lack of blood vessels and markers specific to CD146+ and CD31+. Therefore, based on the results, two possible scenarios suggested for the observed colocalization at the attachment sites are, 1) the cells are already committed to a certain fate or 2) mesenchymal stem cell-like cells of non-pericyte origin. The latter can be identified by using lineage tracing protocols which were beyond the scope of this study. Regardless of origination, the site-specific presence of NG2+ cells had a typical phenotype of osteoblasts and cementoblasts, including polarized and cuboidal shaped cells adjacent to newly formed bone/cementum-like tissue, which was recognized and confirmed by the collagen fibrils. NG2+ cells at the enthesial zones, therefore, can be speculated as progenitors committed to development and mineralization of osteoid matrix, whether or not they are of pericyte origin. However, it should be noted that NG2 is one of the cell-surface proteoglycans known as a surface marker expressed on stem cell populations as well as differentiating chondroblasts, myoblasts, endothelial cells of the brain, and glial progenitors (42, 43). Another hypothetical role of NG2+ cells located at the entheses within bone-PDL-cementum complex is mechanosensation. Sardone et al. (44) showed that when human anterior cruciate ligament (ACL) fibroblasts is subjected to the physiologic stretch, NG2 protein level was moderately increased. In the present study, PDL fibroblasts were stretched due to eruption and masticatory function, which amplified the strain at the PDL insertion site to bone and cementum, and in turn possibly stimulated NG2 expression.

The spatial expression of Osx at entheses was evaluated to confirm the phenotype of the NG2+ cells at the same anatomical locations. The result indicates that periodontal ligament entheses containing enriched subpopulations of NG2+ cells are expected to give rise to tissue-specific cell phenotypes, which are most likely osteoblasts and cementoblasts at the bone-PDL and cementum-PDL attachment sites respectively. To be specific, NG2+/Osx+

cells were intensively populated on active tissue formation sites such as the alveolar bone crests, interradicular bone and secondary cementum. At 3 weeks, when the tooth is not under occlusion yet, but the eruption and root formation of the 2nd mandibular molar had almost finished (45). At this stage, the NG2 and Osx were negative at apical bone-PDL interface (Fig. 4C and 4K, arrowheads), but intense at the secondary cementum surface. Although tooth eruption depends on osteoclastic and blastic activities to generate an eruptive path (46), the last stage of the eruption seems to be driven by cementum apposition rather than bone remodeling or coupling of apical cementum apposition following coronal bone growth. However, 3 months-old mice molars, which have been under functional load, showed NG2+ cell population on both bone-PDL and cementum-PDL interfaces. This result indicates that the PDL-space is maintained during function via cementum apposition as well as bone formation in apical region. Interestingly, this phenomenon was also observed in the interradicular complex. 3 weeks old mice demonstrated little Scx expression in interradicular PDL but abundant vasculature and NG2+ cell population on interradicular bone. This finding implies the driving force for active eruption in the 3 week old lies in the apical and interradicular bone-PDL-cementum complex undergoing differentiation. Interradicular bone of 3 months-old molars was also lined with NG2+/Osx+ cells, which taken together with NG2+/Osx+ cells at apical bone-PDL interface, indicates that with the inception of function, the potential remodeling sites for biomechanical homeostasis are also alveolar crest, interradicular and apical regions.

In addition to site-specificity of cells, the presence and site-specificity of extracellular matrix molecules is equally necessary to provide insights to regenerative mechanisms. BSP, showed no difference in spatial expression along ages and locations except the apical region; BSP was rich on the apical bone-PDL entheses at 3 weeks but not in 3 months (Fig 6 and 7). The lack of BSP immunolabeling on the apical bone-PDL interface at 3 months was opposite to the expected because BSP has been known as mechanosensitive as well as osteogenic and cementogenic molecule (47-49). However, previous *in vitro* studies showed that BSP is also involved in regulation of osteoclast differentiation and activity (50, 51), Osteoclasts and their precursors appear to flow into dental follicle (52, 53) and they adhere to BSP and this interaction plays a regulatory role in their differentiation and activity (54). Little or no BSP expression despite constant stimulation by mechanical load may indicate low bone resorption activity at 3 month and together with NG2/Osx labeling results, led to the conclusion that the position of the root apex in the alveolar socket under physiologic loading condition is maintained by cementum apposition rather than exclusively by bone remodeling. In contrast, increased level of BSP at 3 weeks may facilitate osteoclast activity, which is required for tooth eruption (55, 56).

In the present study, either still erupting (at 3 weeks) or under functional load (at 3 months), the cellular and molecular responses were concentrated at the PDL-alveolar crest, PDL-interradicular bone and apical region of PDL-cementum enthesial zones. Whether the source of mechanical strain is intrinsic (within tissues or cells) or extrinsic (from external environment on a load bearing organ), it plays a role in sculpting and maintaining the organ shape by coordinating the spatial arrangement matrix molecules, cells and controlling cell proliferation and directionality (8, 57). The relative organization of collagen fibers (PSR

staining to enhance collagen birefringence), fibroblasts (scleraxis) and cytoskeleton (phalloidin stained actin filaments) within the PDL representing extracellular matrix (ECM), cells and intracellular structure respectively showed coinciding directionality within PDL except the apical region of 3 weeks old mice. Although the 3 weeks-old molar didn't reach the occlusal plane, the coronal part of the PDL was preferentially orientated with all the three components, indicating that internal erupting force generated by tissue growth and development is dominant in the coronal regions of the periodontal complex. On the other hand, the directionality of collagen birefringence in the apical region at 3 weeks did not coincide with that of PDL fibroblasts and their cytoskeleton. This can be attributed to immature collagen fibrils indicated by low birefringence and sequentially poor coordination of the cells with developing ECM. From this result, therefore, it can be ascertained that physical alterations within intracellular machinery or changes in cell shape is regulated by the mechanical integrity of the extracellular matrix. However, collagen fibers in apical region at 3 weeks had a certain directionality within the complex, which, in turn implicates they were subject to a stretch. Previous *in vitro* studies proved that matrix stiffness regulated osteogenic commitment of MSCs, via traction-dependent adhesion ligand rearrangement (58) and that MSCs specify lineage and commit to phenotypes with extreme sensitivity to tissue-level elasticity (59). Therefore, when the spatial distribution of the biomolecules investigated in this study was reconciled with the cell and matrix directionality, it can be inferred that biophysical signals, especially tensional stretch exerted within the enthesial zones, could be a factor to induce blastic activity at the original enthesis, leading to osteoid and cementoid matrix formation.

Within the context of organ function, the results provide insights to the presence of progenitors and their downstream molecules at the mechanical strained regions such as alveolar crests, interradicular and apical regions. Additionally, relevant biophysical signals should be considered for regenerating matrices at both stages of development and function of organs. Calibrated tuning of matrix stretch over time can result in functional quality necessary to maintain the dynamic entheses at ligament-bone and ligament-cementum attachment sites in load-bearing bone-PDL-tooth fibrous joints.

Supplementary Material

Refer to Web version on PubMed Central for supplementary material.

Acknowledgments

The authors thank Nikon Imaging Center (NIC) at UCSF for their facility and assistance in fluorescence microscopy. We also thank Dr. William Landis and Ms. Robin Jacquet at University of Akron, Dr. Marian Young at NIH/NIDCR for their insights in the data analysis and interpretation, Ms. Linda Prentice for her help in specimen preparation and Dr. Jing Du for technical assistance in quantification analysis. This research was supported by NIH/NIDCR R01DE022032 (SPH) and the Department of Preventive and Restorative Dental Sciences, UCSF and the Department of Orofacial Sciences, UCSF.

References

1. Lu HH, Thomopoulos S. Functional attachment of soft tissues to bone: development, healing, and tissue engineering. Annual review of biomedical engineering. 2013; 15:201.

2. Benjamin M. Anatomy and biochemistry of entheses. Annals of the rheumatic diseases. 2000; 59:995–999.
3. Galatz L, Rothermich S, VanderPloeg K, Petersen B, Sandell L, Thomopoulos S. Development of the supraspinatus tendon-to-bone insertion: Localized expression of extracellular matrix and growth factor genes. Journal of Orthopaedic Research. 2007; 25:1621–1628. [PubMed: 17600822]
4. Benjamin M, Toumi H, Ralphs J, Bydder G, Best T, Milz S. Where tendons and ligaments meet bone: attachment sites ('entheses') in relation to exercise and/or mechanical load. Journal of anatomy. 2006; 208:471–490. [PubMed: 16637873]
5. Benjamin M, McGonagle D. Entheses: tendon and ligament attachment sites. Scandinavian journal of medicine & science in sports. 2009; 19:520–527. [PubMed: 19522749]
6. Weinman JP, Sicher H. Bone and bones. Fundamentals of bone biology. The American Journal of the Medical Sciences. 1948; 215:113.
7. Kraw AG, Enlow DH. Continuous attachment of the periodontal membrane. American Journal of Anatomy. 1967; 120:133–147.
8. Ingber DE. Mechanical control of tissue morphogenesis during embryological development. International Journal of Developmental Biology. 2006; 50:255. [PubMed: 16479493]
9. Thomopoulos S, Genin GM, Galatz LM. The development and morphogenesis of the tendon-to-bone insertion What development can teach us about healing. Journal of musculoskeletal & neuronal interactions. 2010; 10:35. [PubMed: 20190378]
10. Mammoto T, Ingber DE. Mechanical control of tissue and organ development. Development. 2010; 137:1407–1420. [PubMed: 20388652]
11. Blitz E, Viukov S, Sharir A, et al. Bone Ridge Patterning during Musculoskeletal Assembly Is Mediated through SCX Regulation of *Bmp4* at the Tendon-Skeleton Junction. Developmental cell. 2009; 17:861–873. [PubMed: 20059955]
12. Johnson K. A study of the dimensional changes occurring in the maxilla following tooth extraction*. Australian Dental Journal. 1969; 14:241–244. [PubMed: 5259350]
13. Kuboki Y, Hashimoto F, Ishibashi K. Time-dependent changes of collagen crosslinks in the socket after tooth extraction in rabbits. Journal of Dental Research. 1988; 67:944–948. [PubMed: 3170907]
14. Pryce BA, Brent AE, Murchison ND, Tabin CJ, Schweitzer R. Generation of transgenic tendon reporters, ScxGFP and ScxAP, using regulatory elements of the scleraxis gene. Developmental Dynamics. 2007; 236:1677–1682. [PubMed: 17497702]
15. Feng B, Zhang D, Kuriakose G, Devlin CM, Kockx M, Tabas I. Niemann-Pick C heterozygosity confers resistance to lesional necrosis and macrophage apoptosis in murine atherosclerosis. Proceedings of the National Academy of Sciences. 2003; 100:10423–10428.
16. Lee JH, Lin JD, Fong JI, Ryder MI, Ho SP. The Adaptive Nature of the Bone-Periodontal Ligament-Cementum Complex in a Ligature-Induced Periodontitis Rat Model. BioMed research international. 2013; 2013
17. Nakashima K, Zhou X, Kunkel G, et al. The novel zinc finger-containing transcription factor osterix is required for osteoblast differentiation and bone formation. Cell. 2002; 108:17–29. [PubMed: 11792318]
18. Zhou X, Zhang Z, Feng JQ, et al. Multiple functions of Osterix are required for bone growth and homeostasis in postnatal mice. Proceedings of the National Academy of Sciences. 2010; 107:12919–12924.
19. Hirata A, Sugahara T, Nakamura H. Localization of runx2, osterix, and osteopontin in tooth root formation in rat molars. Journal of Histochemistry & Cytochemistry. 2009; 57:397–403. [PubMed: 19124839]
20. Cao Z, Zhang H, Zhou X, et al. Genetic evidence for the vital function of Osterix in cementogenesis. Journal of Bone and Mineral Research. 2012; 27:1080–1092. [PubMed: 22246569]
21. Inoue M, Ebisawa K, Itaya T, et al. Effect of GDF-5 and BMP-2 on the expression of tendo/ligamentogenesis-related markers in human PDL-derived cells. Oral diseases. 2012; 18:206–212. [PubMed: 22093095]

22. Lindhe, J.; Lang, NP.; Karring, T. Clinical periodontology and implant dentistry. John Wiley & Sons; 2009.
23. Kristensen HB, Andersen TL, Marcussen N, Rolighed L, Delaisse JM. Increased presence of capillaries next to remodeling sites in adult human cancellous bone. J Bone Miner Res. 2013; 28:574–585. [PubMed: 22991221]
24. Chen SC, Marino V, Gronthos S, Bartold PM. Location of putative stem cells in human periodontal ligament. Journal of Periodontal Research. 2006; 41:547–553. [PubMed: 17076780]
25. Crisan M, Yap S, Casteilla L, et al. A perivascular origin for mesenchymal stem cells in multiple human organs. Cell Stem Cell. 2008; 3:301–313. [PubMed: 18786417]
26. Roguljic H, Matthews B, Yang W, Cvija H, Mina M, Kalajzic I. In vivo identification of periodontal progenitor cells. Journal of dental research. 2013; 92:709–715. [PubMed: 23735585]
27. Feng J, Mantesso A, De Bari C, Nishiyama A, Sharpe PT. Dual origin of mesenchymal stem cells contributing to organ growth and repair. Proceedings of the National Academy of Sciences of the United States of America. 2011; 108:6503–6508. [PubMed: 21464310]
28. Zhao H, Feng J, Seidel K, et al. Secretion of Shh by a Neurovascular Bundle Niche Supports Mesenchymal Stem Cell Homeostasis in the Adult Mouse Incisor. Cell stem cell. 2014; 14:160–173. [PubMed: 24506883]
29. Crisan M, Yap S, Casteilla L, et al. A perivascular origin for mesenchymal stem cells in multiple human organs. Cell stem cell. 2008; 3:301–313. [PubMed: 18786417]
30. Sorrentino A, Ferracin M, Castelli G, et al. Isolation and characterization of CD146+ multipotent mesenchymal stromal cells. Experimental hematology. 2008; 36:1035–1046. [PubMed: 18504067]
31. Seo BM, Miura M, Gronthos S. Investigation of multipotent postnatal stem cells from human periodontal ligament. Lancet. 2004; 364:1756–1756.
32. Xu J, Wang W, Kapila Y, Lotz J, Kapila S. Multiple differentiation capacity of STRO-1+/CD146+ PDL mesenchymal progenitor cells. Stem cells and development. 2008; 18:487–496. [PubMed: 18593336]
33. Lin NH, Menicanin D, Mrozik K, Gronthos S, Bartold P. Putative stem cells in regenerating human periodontium. Journal of periodontal research. 2008; 43:514–523. [PubMed: 18624941]
34. Ozerdem U, Grako KA, Dahlin-Huppe K, Monosov E, Stallcup WB. NG2 proteoglycan is expressed exclusively by mural cells during vascular morphogenesis. Developmental Dynamics. 2001; 222:218–227. [PubMed: 11668599]
35. Iwasaki K, Komaki M, Yokoyama N, et al. Periodontal ligament stem cells possess the characteristics of pericytes. Journal of periodontology. 2012:1–16.
36. Freezer S, Sims M. A transmission electron-microscope stereological study of the blood vessels, oxytalan fibres and nerves of mouse-molar periodontal ligament. Archives of oral biology. 1987; 32:407–412. [PubMed: 3479081]
37. Miller N. Ten Cate's oral histology. British Dental Journal. 2012; 213:194–194.
38. Karsenty G, Wagner EF. Reaching a genetic and molecular understanding of skeletal development. Developmental cell. 2002; 2:389–406. [PubMed: 11970890]
39. Li J, Sarosi I, Yan XQ, et al. RANK is the intrinsic hematopoietic cell surface receptor that controls osteoclastogenesis and regulation of bone mass and calcium metabolism. Proceedings of the National Academy of Sciences. 2000; 97:1566–1571.
40. Bosshardt D. Are cementoblasts a subpopulation of osteoblasts or a unique phenotype? Journal of dental research. 2005; 84:390–406. [PubMed: 15840773]
41. Grzesik WJ, Narayanan AS. Cementum and periodontal wound healing and regeneration. Critical Reviews in Oral Biology & Medicine. 2002; 13:474–484. [PubMed: 12499241]
42. Fukushi, Ji; Inatani, M.; Yamaguchi, Y.; Stallcup, WB. Expression of NG2 proteoglycan during endochondral and intramembranous ossification. Developmental dynamics. 2003; 228:143–148. [PubMed: 12950088]
43. Esko, J.; Kimata, K.; Lindahl, U. Essentials of Glycobiology. 2nd. Cold Spring Harbor (NY): Cold Spring Harbor Laboratory Press; 2009.

44. Sardone F, Traina F, Tagliavini F, et al. Effect of Mechanical Strain on the Collagen VI Pericellular Matrix in Anterior Cruciate Ligament Fibroblasts. Journal of cellular physiology. 2014; 229:878–886. [PubMed: 24356950]
45. Shibata S, Suzuki S, Tengan T, Yamashita Y. A histochemical study of apoptosis in the reduced ameloblasts of erupting mouse molars. Archives of oral biology. 1995; 40:677–680. [PubMed: 7575241]
46. Wise G, Frazier-Bowers S, D'souza R. Cellular, molecular, and genetic determinants of tooth eruption. Critical Reviews in Oral Biology & Medicine. 2002; 13:323–335. [PubMed: 12191959]
47. MacNeil R, Berry J, D'errico J, Strayhorn C, Piotrowski B, Somerman M. Role of two mineral-associated adhesion molecules, osteopontin and bone sialoprotein, during cementogenesis. Connective tissue research. 1995; 33:1–7. [PubMed: 7554941]
48. Carvalho R, Bumann A, Schaffer J, Gerstenfeld L. Predominant integrin ligands expressed by osteoblasts show preferential regulation in response to both cell adhesion and mechanical perturbation. Journal of cellular biochemistry. 2002; 84:497–508. [PubMed: 11813255]
49. Foster B, Soenjaya Y, Nociti F, et al. Deficiency in Acellular Cementum and Periodontal Attachment in Bsp Null Mice. Journal of dental research. 2013; 92:166–172. [PubMed: 23183644]
50. Raynal C, Delmas PD, Chenu C. Bone sialoprotein stimulates in vitro bone resorption. Endocrinology. 1996; 137:2347–2354. [PubMed: 8641185]
51. Malaval L, Wade-Guéye NM, Boudiffa M, et al. Bone sialoprotein plays a functional role in bone formation and osteoclastogenesis. The Journal of experimental medicine. 2008; 205:1145–1153. [PubMed: 18458111]
52. Marks SC, Cahill DR, Wise GE. The cytology of the dental follicle and adjacent alveolar bone during tooth eruption in the dog. American journal of anatomy. 1983; 168:277–289. [PubMed: 6650440]
53. Volejnikova S, Laskari M, Marks SC Jr, Graves DT. Monocyte recruitment and expression of monocyte chemoattractant protein-1 are developmentally regulated in remodeling bone in the mouse. The American journal of pathology. 1997; 150:1711. [PubMed: 9137095]
54. Nakamura I, Duong LT, Rodan SB, Rodan GA. Involvement of αvβ3 integrins in osteoclast function. Journal of bone and mineral metabolism. 2007; 25:337–344. [PubMed: 17968485]
55. Sundquist KT, Marks SC. Bafilomycin A1 inhibits bone resorption and tooth eruption in vivo. Journal of Bone and Mineral Research. 1994; 9:1575–1582. [PubMed: 7817803]
56. Cielinski MJ, Jolie M, Wise GE, Marks SC. The contrasting effects of colony-stimulating factor-1 and epidermal growth factor on tooth eruption in the rat. Connective tissue research. 1995; 32:165–169. [PubMed: 7554913]
57. Nelson CM, Gleghorn JP. Sculpting organs: mechanical regulation of tissue development. Annual review of biomedical engineering. 2012; 14:129–154.
58. Huebsch N, Arany PR, Mao AS, et al. Harnessing traction-mediated manipulation of the cell/matrix interface to control stem-cell fate. Nature materials. 2010; 9:518–526. [PubMed: 20418863]
59. Engler AJ, Sen S, Sweeney HL, Discher DE. Matrix Elasticity Directs Stem Cell Lineage Specification. Cell. 2006; 126:677–689. [PubMed: 16923388]

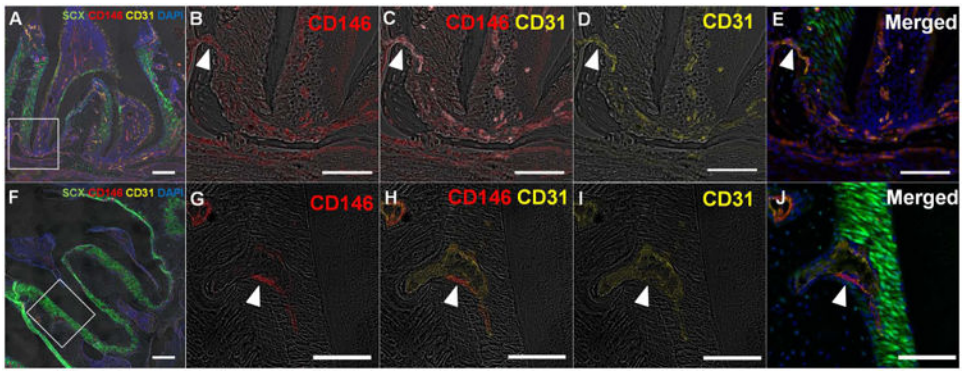

Figure 1. Co-immunofluorescent staining of CD146 with endothelial cell marker, CD31 in scxGFP mouse 2nd molar at 3 weeks (A-E) and 3 months (F-J) of age

(A, F) CD146+ cells were detected in association with vasculature identified by CD31, through subginigival connective tissue, PDL space, dental pulp, endosteal space, and bone marrow. **(B-E, G-J)** Magnified view of the inserted insets in panel A and F. CD146+ cells are derived from endosteal spaces through the channels between alveolar bone and PDL (arrowhead). Scale bar; 200μm (A,F), 100μm (B-E, G-J)

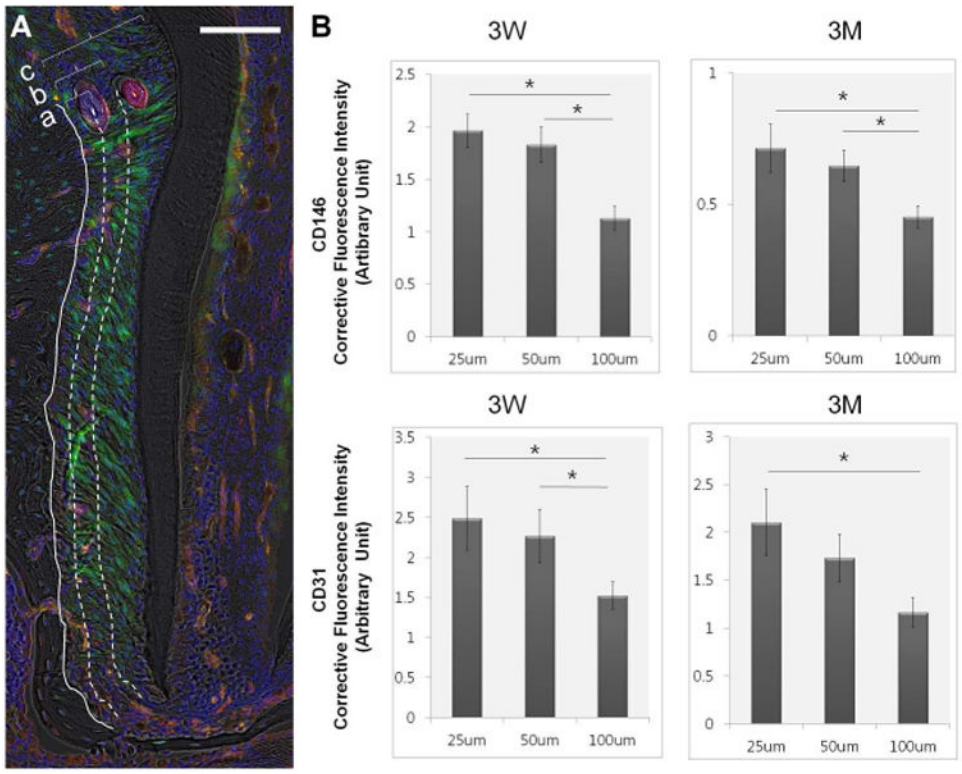

Figure 2. The distribution of CD 146+, CD31+ Cells in the vicinity of bone-PDL interface

(A) The fluorescent intensity of CD146 and CD31 was measured within 25μm (a), 50μm (b), and 100μm (c) from B to PDL interface of mesial complex of mandibular 2nd molar, Scale bar=100μm. **(B)** Both CD31 and CD146 showed significantly higher fluorescence within 25μm and 50μm compared to 100μm at both ages * statistically significance ($p<0.05$), N=5, error bars present the standard error of the mean (SEM)

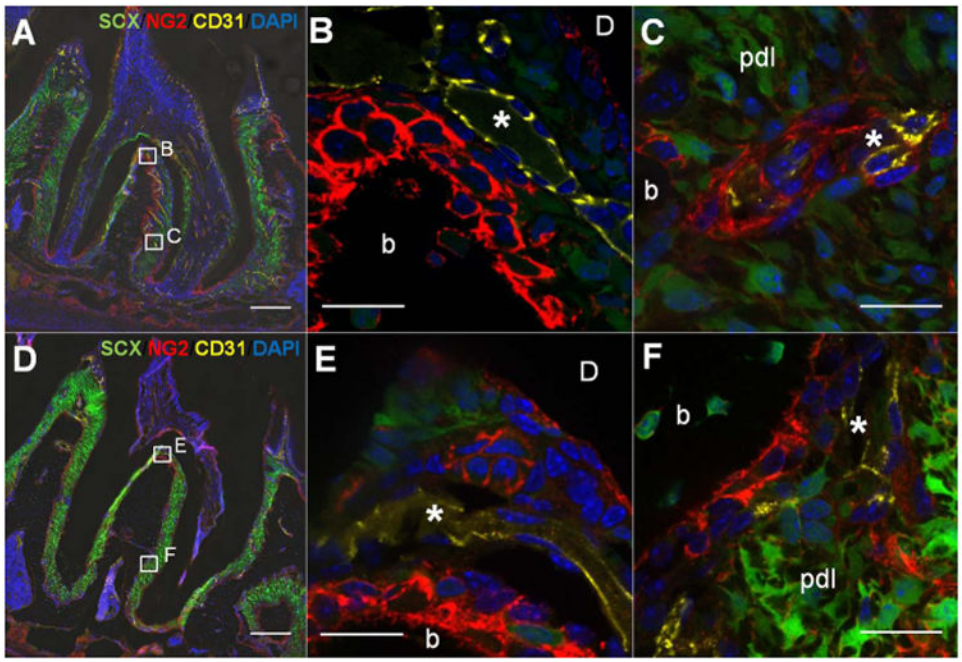

Figure 3. Co-immunofluorescent staining of NG2+ cells with endothelial cell marker, CD31 in scxGFP mouse 2nd molar at 3 weeks (A-C) and 3 months (D-F) of age

(A,D at X20) NG2+ cells (red) were observed in proximity of CD31+ blood vessels (yellow) but also at bone-PDL and cementum-PDL interfaces. **(B, E at X60)** Magnified view of interradicular region. Interradicular region was intensely populated with CD31+ blood vessels (*) closely to NG2+ cell-lining bone-PDL interface. **(C, F at X60)** PDL adjacent to bone. NG2+ cells are located adjacent to CD31+ endothelial wall (*) within PDL. b=bone, d=dentin, Scale bar; 200μm (A, D), 20μm (B,C,E and F)

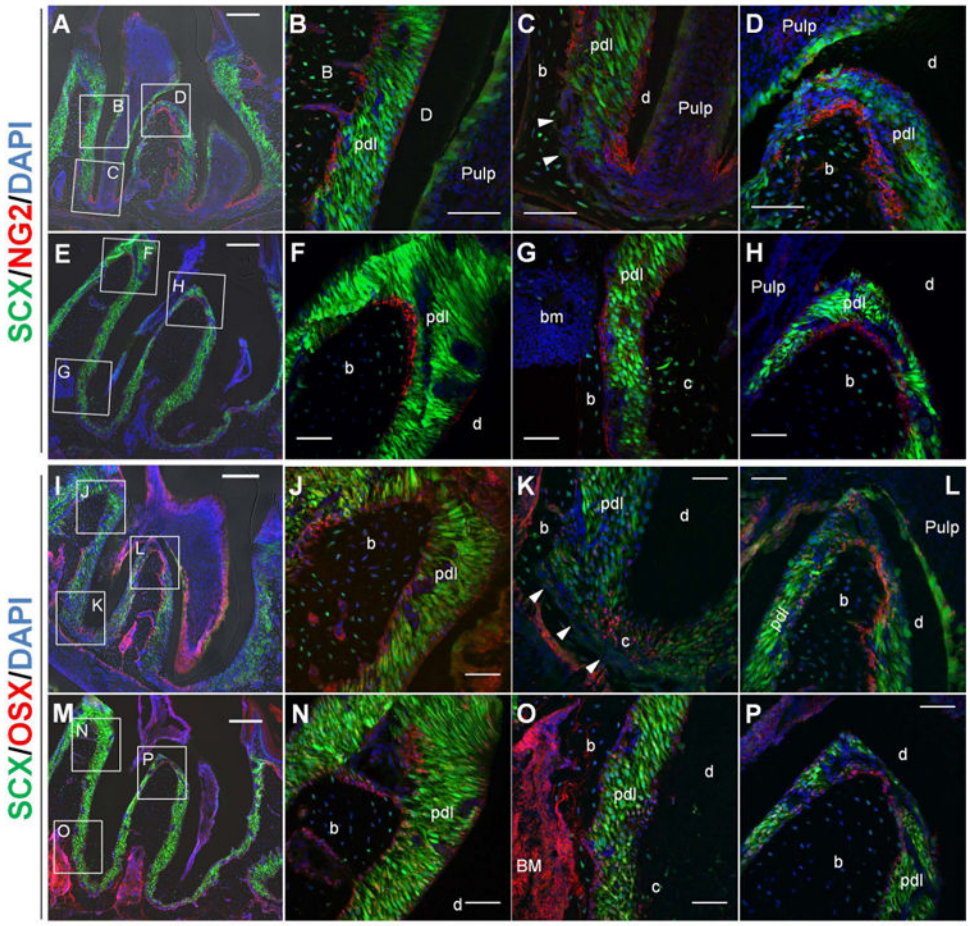

Figure 4. Immunofluorescent localization of NG2+ (A-H) and Osx+ (I-P) cells in scxGFP mouse 2nd molar at 3 weeks (A-D and I-L) and 3 months (E-H and M-P) of age

(A-H) NG+ cells (red) were observed along bone-PDL and cementum-PDL interfaces. Bone-PDL interface had NG2+ cells coronally (B, D) but not apically (C, arrowheads), although 3 months-old mice showed increased NG expression in apical region (G) as well as on alveolar crest (F) and interradicular bone (H). On the other hand, NG+ cells at cementum-PDL interface of 3 weeks-old mice, were concentrated in the region where cellular cementum is actively developing (C). This pattern was also observed in 3 months-old mice but not as obvious as in 3 weeks-old mice. **(I-P)** Osx+ cells (red or pink) were detected at the location of NG2+ cells along interface: bone-PDL attachment site (J,L,N and P) except apical bone-PDL interface (K, arrowheads) and cementum-PDL interface (K, O). Moreover, Osx was positive in odontoblasts lining pulp chamber and root canal (I and M), bone marrow stromal cells (I,M and O) and some Scx+ PDL fibroblasts. b=bone, d=dentin, c=cementum, bm=bone marrow, Scale bar=200um (A,E,I and M), 50um (B-D, F-H, J-L, and N-P)

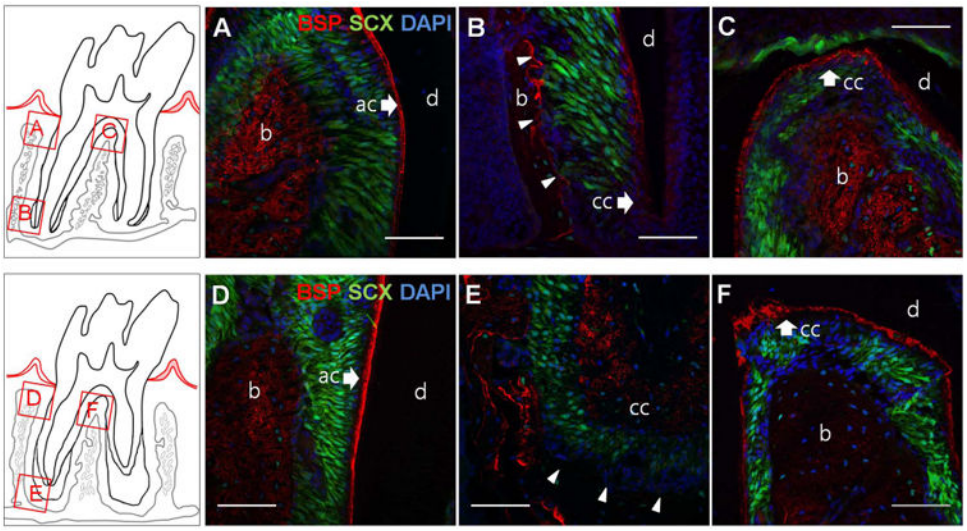

Figure 5. Immunofluorescence of BSP in scxGFP mouse 2nd molar at 3 weeks (A-C) and 3 months (D-F) of age

BSP (red) is localized to alveolar bone (b), acellular cementum (ac) and cellular cementum (cc) at both ages. BSP was evenly distributed in coronal region (A,D) and interradicular bone (C,F) with a rich expression in cement lines of apical bone (B,E), However, BSP is enriched at the apical bone-PDL interface at 3 weeks (B, arrowheads), whereas the apical bone-PDL interface at 3 months is BSP negative (E, arrowheads). b= alveolar bone, d=dentin, ac=acellular cementum, cc =cellular cementum, Scale bar = 50μm

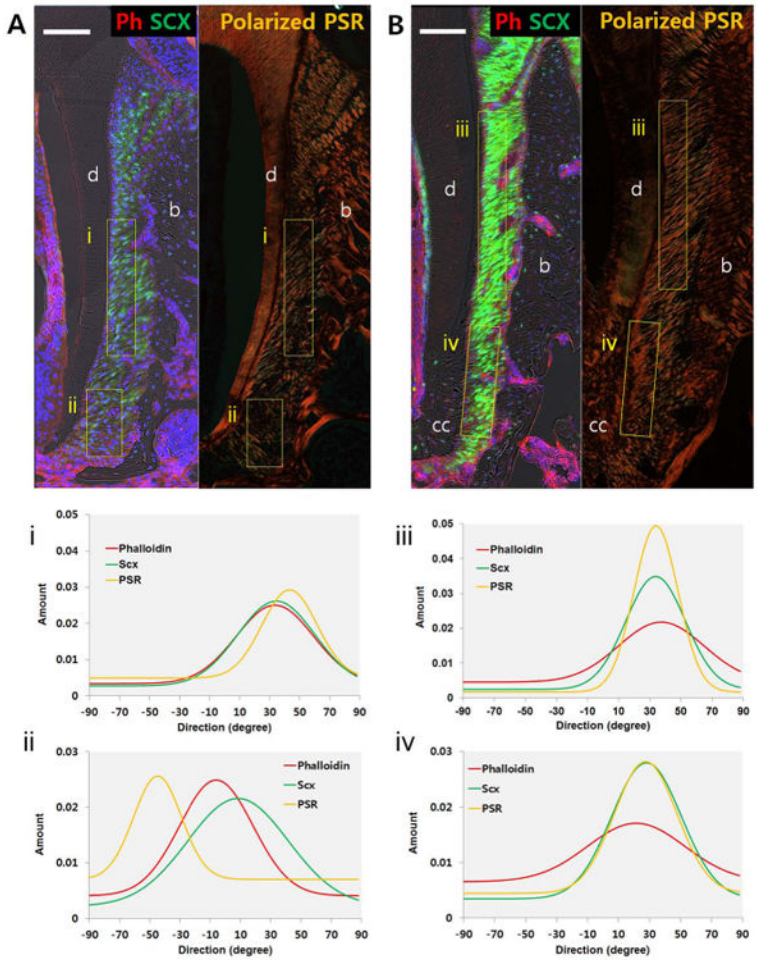

Figure 6. Orientation and organization of PDL cell cytoskeleton, fibroblasts and collagen fibers

Immunofluorescence of phalloidin (red) and polarized light microscopy of PSR staining in scxGFP 2nd molar at 3 weeks (A) and 3 months (B). Plots illustrate directionality of birefringent collagen fibers, fibroblasts, and PDL cell cytoskeletons within mesiocoronal (i,iii) and mesioapical regions (ii,iv). Directionality of collagen fibers, fibroblasts, and PDL cell cytoskeleton coincides within PDL complex, except in apical region of 3 weeks old group. b=alveolar bone, d=dentin, cc=cellular cementum, Scale bar = 100μm

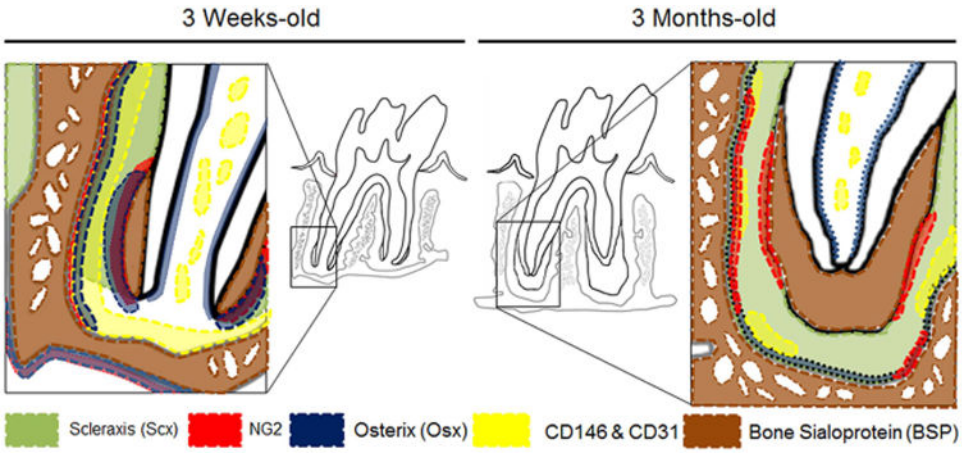

Figure 7. Schematic representation of the distribution of biomolecules identified in scxGFP mice molar at 3 weeks and 3 months

The alveolar bone crest and periapical region are areas of high biomechanical activity and the entheses within those regions are putative locations of cellular differentiation and tissue adaptation. Perivascular niche for stemness identified using CD146 and CD31 (yellow) runs along bone-PDL entheses. NG2/Osx+ cells line the bone-PDL and cementum-PDL entheses, where biophysical signals from eruption and function are supposedly amplified. Scx are positive only in the fully developed PDL as a conveyer of biophysical cues. BSP was rich at apical bone-PDL enthesis at 3 weeks but negative at 3 months